PAPER

Compact implementation of high-dimensional mutually partially unbiased bases protocol

To cite this article: Zehong Chang *et al* 2023 *Quantum Sci. Technol.* **8** 035028

Quantum Science and Technology

PAPER

Compact implementation of high-dimensional mutually partially unbiased bases protocol

Zehong Chang[1], Yunlong Wang[1], Zhenyu Guo[1], Min An[1], Rui Qu[1], Junliang Jia[1], Fumin Wang[1,2,*] and Pei Zhang[1,3,*]

[1] Ministry of Education Key Laboratory for Nonequilibrium Synthesis and Modulation of Condensed Matter, Shaanxi Province Key Laboratory of Quantum Information and Quantum Optoelectronic Devices, School of Physics, Xi'an Jiaotong University, Xi'an 710049, People's Republic of China
[2] National Local Joint Engineering Research Center for Precision Surgery & Regenerative Medicine, Shaanxi Provincial Center for Regenerative Medicine and Surgical Engineering, The First Affiliated Hospital of Xi'an Jiaotong University, Xi'an, Shaanxi Province 710061, People's Republic of China
[3] State Key Laboratory of Applied Optics, Changchun Institute of Optics, Fine Mechanics and Physics, Chinese Academy of Sciences, Changchun 130033, People's Republic of China
* Authors to whom any correspondence should be addressed.

E-mail: wh2009616@163.com and zhangpei@mail.ustc.edu.cn

RECEIVED
14 November 2022

REVISED
24 April 2023

ACCEPTED FOR PUBLICATION
12 June 2023

PUBLISHED
20 June 2023

Keywords: quantum optics, quantum cryptography, quantum key distribution, transverse spatial modes, high-dimensional

Abstract

Transverse spatial mode of light is crucial in high-dimensional quantum key distribution (QKD). However, applications in realistic scenarios suffer from mode-dependent loss and the complexity of system, making it impractical to achieve higher-dimensional, longer-distance and low-cost communications. A mutually partially unbiased bases (MPUBs) protocol has been proposed to fundamentally eliminate the effects induced by mode-dependent loss for long propagation distances and limited sizes of apertures. Here, we demonstrate the first implementation of the MPUBs protocol in dimensions of $d = 2, 4, 5$ and 6. By performing a controlled unitary transformation, we can actively switch the measurement basis and enable a compact measurement system. In consequence, a higher encoding dimension is available under finite system resources, resulting in higher key rates and stronger noise resistance. Our work enhances the practicability of MPUBs protocol, and may promote the applications of high-dimensional QKD in quantum networks.

1. Introduction

Quantum key distribution (QKD) is a crucial procedure towards information-theoretic secure communication between two remote users, Alice and Bob, and is arguably the fastest-growing area in quantum information science [1–7]. High-dimensional QKD has been a rising interest in recent years, due to the increased information capacity and enhanced robustness to noise [8–11]. Different degrees of freedom (DoF) of the photon provide abundant options for expanding Hilbert space to implement high-dimensional QKD. The orbital angular momentum (OAM) of light [12, 13], as a subset of transverse spatial modes, becomes a powerful candidate to implement high-dimensional QKD, featuring infinite dimensional Hilbert space [14, 15]. Indeed, the properties of different mode families can also be exploited to enhance the performance in various application scenarios [16–21]. So far, high-dimensional QKD using transverse spatial modes has been demonstrated over a 300 m free-space link [22], a 1.2 km optical fiber [23] and a 3 m underwater link [24].

However, the encoding dimension in current outdoor experiments is below ($d \leqslant 4$) as well as a limited transmission distance in free space. The main reason is the severe performance decline during transmission arising from mode-dependent beam diffraction and accumulated propagation phase [25]. The divergence of spatial modes scales as $\sqrt{N+1}$, where N refers to mode order [26]. Thus, the states in the computational

basis (e.g. OAM states) will suffer from mode-dependent loss owing to the limited optical apertures in practical links. It also occurs for states in the Fourier basis which are made up of an equal superposition of OAM states with a fixed relative phase between adjacent OAM states. Even in the absence of turbulence, these relative phases will vary because of the mode-dependent accumulated propagation phase (e.g. the Gouy phase [27, 28], which also scales to $N+1$). Eventually, implementing a higher-dimensional and longer-distance QKD becomes impractical.

To overcome the above issues, Zhao *et al* proposed a waist pre-compensation protocol by balancing the efficiencies of different mode order quantum states [25]. The protocol is universal but requires real-time feedback and adjustment in case of variable communication distance, such as handheld devices [29], satellites [30] and drone [31] platforms. Another approach proposed by Wang *et al* adopted the same order quantum states from Laguerre–Gaussian (LG) and Hermite-Gaussian (HG) mode families to encode information [32]. The states between the two mode families are not mutually unbiased, thus the approach is called the mutually partially unbiased bases (MPUBs) protocol. Although the maximum tolerable error rate is reduced compared to the fully mutually unbiased bases (MUBs)-based protocol, the protocol can eliminate mode-dependent problems and break the boundary in applications. At present, the protocol has not been demonstrated experimentally.

Regarding the practical applications, the complexity of systems (especially in the detection system) increases as the encoding dimension, thereby the cost to implement QKD is raised [33]. Also, the accurate characterization of devices to avoid security loopholes becomes complicated [1, 5]. A compact measurement scheme designed for high-dimensional QKD is essential [34]. In this work, we first proposed a compact scheme for MPUBs protocol, where the polarization DoF is introduced as a control bit to enable switching of the measurement basis. Thus, only one-half of mode sorters and detectors are required compared with the passive measurement scheme. Then, we implemented a proof-of-principle experiment for the MPUBs protocol in dimensions of $d=2,4,5,6$, and verified the practicability of this compact scheme. Finally, we theoretically analyzed the effects induced by basis-dependent detection flaw [35] in the implementation of high-dimensional QKD. Our scheme shows potential for detecting or closing this flaw owing to the simple setup. Our work may contribute to promoting the applications of high-dimensional QKD.

2. Theory

The MPUBs protocol encodes the information in transverse spatial modes of light. However, as opposed to the other protocols that only utilize the OAM of spatial modes, the MPUBs protocol exploits all DoF to guarantee the same divergence angle as well as the accumulated propagation phase [25]. This allows the MPUBs protocol to improve the secret key rate in an intra-city network scenario (in terms of long propagation distances and limited sizes of apertures), while at the same time enhancing robustness against channel noise.

In the MPUBs protocol, two complementary encoding bases correspond to the LG and 45° HG modes families in transverse spatial modes, characterised by $|l,p\rangle$ and $|n,m\rangle$, respectively. Here $\{l,p,n,m\}$ refer to modes indices. The two kinds of spatial modes can be written in the circular coordinates (r,ϕ) and Cartesian coordinate (x,y), respectively,

$$\langle r,\phi|l,p\rangle = A_{LG}\left(\frac{\sqrt{2}r}{w}\right)^{|l|} L_p^l\left(\frac{2r^2}{w^2}\right) e^{-r^2/w^2} e^{il\phi}, \tag{1}$$

$$\langle x,y|n,m\rangle = A_{HG} H_n\left(\frac{x-y}{w}\right) H_m\left(\frac{x+y}{w}\right) e^{-(x^2+y^2)/w^2}, \tag{2}$$

where $A_{LG}=\sqrt{\frac{2p!}{\pi w^2(p+|l|)!}}$ and $A_{HG}=\sqrt{\frac{1}{\pi w^2 n!m!2^{n+m-1}}}$ are the normalized coefficients. w is the beam waist, $L_p^l(\cdot)$ donates the generalized Laguerre polynomial and $H_n(\cdot)$ is the Hermite polynomial of order n. The mode order is defined by $N=2p+|l|=n+m$, where $\{p,n,m\}$ is a nonnegative integer and l is a integer.

For a d-dimensional MPUBs protocol, the encoding states can be represented by $\{|l_i\rangle=|l,p\rangle, |h_i\rangle=|n,m\rangle\}$, with $i\in[0,\ d-1]$ and $d=N+1$. Two bases are called MPUBs because the inner product of any vector from the first basis with any vector from the second basis satisfies $|\langle l_i|h_j\rangle|^2\neq 1/d$. When the transmitter, usually called Alice, has prepared the quantum states, she sends them through an insecure channel towards the receiver, called Bob. It is straightforward for Bob to measure the states in LG basis with a LG mode sorter [36–41]. However, the development of HG mode sorter is far from mature [42]. Fortunately, a $\pi/2$ mode converter [43–45] can efficiently convert states in HG basis into corresponding states in the LG basis, and vice versa. A sequence of $\pi/2$ mode converter and LG sorter can enables the projection

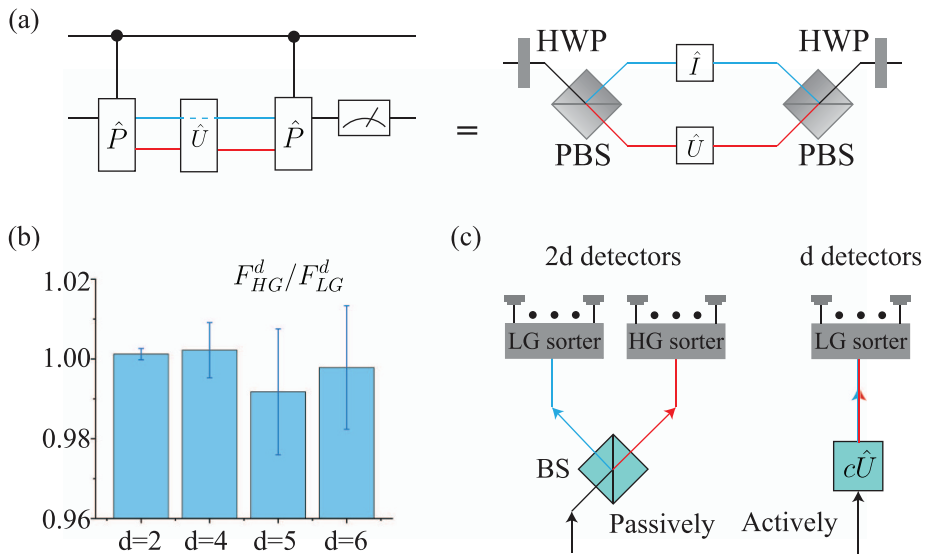

Figure 1. (a) Logic circuit of a $c\hat{U}$ gate and the optical schematic for implementing a compact MPUBs protocol. Half-wave plate (HWP); polarizing beam splitter (PBS). (b) Efficiency of the unitary transformation $\hat{U}$ in different dimensions. (c) Visible demonstration of the benefit for compact (active measurement) versus passive measurement schemes.Beam splitter (BS).

measurement in HG basis. The unitary transformation $\hat{U}$ performed by the mode converter is valid in different dimensions. The elements are given by

$$U_{\mu,j} = \sum_{k=0}^{N} i^k b(\mu, N-\mu, k) b(j, N-j, k), \tag{3}$$

with real coefficients

$$b(n,m,k) = \sqrt{\frac{(N-k)!k!}{2^N n!m!}} \frac{1}{k!} \frac{d^k}{dt^k} [(1-t)^n (1+t)^m]_{t=0}, \tag{4}$$

where the integer number $\{\mu, j, k\} \in [0, N]$.

Similar to most transverse spatial modes encoding protocols, a beam splitter (BS) randomly and passively selects measurement basis in the original MPUBs protocol. One main reason is that mapping between different bases remains challenging, due to the immature high-dimensional quantum gate technology [46–48]. One corresponding issue for this passive scheme is that the number of devices required for the measurement makes the deployment of higher-dimensional protocol impractical. To implement a compact setup, we construct a controlled unitary transformation, called c$\hat{U}$ gate, to actively switch the measurement basis. We take the two-dimensional polarization DoF as a controlled qubit, while the target qudit corresponds to the arbitrary-dimensional transverve spatial modes. The mathematical representation of the transformation can be formulated as follows:

$$c\hat{U} = |H\rangle\langle H| \otimes \hat{U} + |V\rangle\langle V| \otimes \hat{I}, \tag{5}$$

where $|H\rangle$ and $|V\rangle$ are eigenstates of two-dimensional Pauli matrix σ_Z. A logic circuit shows in figure 1(a). The circuit is composed of three parts: controlled-path ($c\hat{P}$) gates at the beginning, which move the target qubits from upper path (labelled blue) to lower path (labelled red) according to the control qubit. The unitary transformation $\hat{U}$ in the middle is implemented on the lower path, and a $c\hat{P}$ at the end combines the upper and lower paths. In the optical schematic, we use the combination of half-wave plate (HWP) and polarization beam splitter (PBS) to construct the $c\hat{P}$ gate. The last HWP makes the polarization of the photons from both paths the same. Figure 1(b) displays the efficiencies to perform unitary transformation $\hat{U}$ in different dimensions. The main experimental error derives from the waist mismatching in the higher-order transverse spatial modes.

The core advantage is that only one-half of mode sorters and detectors are required in the detection system, as shown in figure 1(c). Consequently, it allows for the implementation of a MPUBs protocol in a dimension twice as great as that of a solely OAM based protocol. The ability to increase encoding dimension

lowers the threshold on the quantum bit error rate (QBER) needed to execute QKD securely and enables the use of lower-quality devices. On the other hand, the requirement for calibration of measurement devices can be mitigated, making it easier to close or analyze the side information in the detection system, such as detection efficiency mismatch [49] and basis-dependent detection flaw [35].

3. Experimental setup

A principle-and-proof experiment is implemented to verify the performance of MPUBs protocol, as shown in figure 2. A 405 nm continuous wave laser beam is coupled to a single-mode fibre (SMF) to obtain a pure fundamental Gaussian mode pump beam. The single photon pairs, namely signal and idler, are generated through type-II spontaneous parametric down-conversion process (SPDC) in a 5-mm-long periodically poled potassium titanyl phosphate (PPKTP) crystal. After the PBS, the polarization orthogonal correlated photon pairs are separated. The generated photon pairs are coupled to SMF in order to filter their spatial modes to the fundamental mode. Following the SMF, a coincidence rate of 63 kHz is measured within a coincidence time window of 1.5 ns. The heralded signal photon is sent onto SLM1 corresponding to Alice's generation stage. The SLM (HDSLM80R-plus, UPOLabs) are electronically controlled nematic liquid crystal devices with 1920×1200 pixels, a refresh rate of 60 Hz and diffraction efficiency in excess of 70%. The encoding states are produced using a phase-only holography technique [50]. Alice's heralded photon with horizontal polarization is subsequently sent over the untrusted quantum channel.

The received states are measured by two measurement setups. The first setup corresponds to the passive measurement scheme. The photons pass only through path1 by setting the two HWPs at 45°. The second setup corresponds to our compact measurement scheme. Bob randomly and independently switches the measurement basis by rotating the angles of two HWPs both to either $\theta = 0°$ or 45°, guiding the photons in two paths. In experiments, two-axes stage controllers (GSC-02), featuring stepping motor drivers, are employed to perform the active rotation. An integrated $\pi/2$ mode converter in path2 is used to realize unitary transformation. Then, Bob uses his SLM2 followed by a SMF to perform a projection. In order to do so, Bob uses the flattening technique [51] to perform generalized projective measurements. If the incoming photon carried the mode corresponding to Bob's projection, the mode is flattened and the photon will couple to the SMF. Long-pass optical filters are used to reduce the detection of noise photons. Coincidences are recorded using single-photon avalanche detectors (ID120-500-800nm, ID Quantique) with a dark count rate of less than 50 Hz and a measured dead time of approximately 400 ns.

In our proof-of-principle experiment, the number of holograms loaded onto SLM2 corresponds to the required number of detectors in a realistic system. In addition, the different mode families to which the holograms belong are indicative of the number of mode sorters required. To quantitatively show the performance, we measure the conditional probability of finding each state received by Bob for each state transmitted by Alice, and display the results in a crosstalk matrix. For each permutation of encoding states by Alice and projective measurements by Bob, the single count rates and coincidence count rates are recorded and the normalized joint probabilities.

As a comparison, figures 3(b) and (c) show the crosstalk matrices obtained for the two-dimensional BB84 and six-state protocols. Four and six holograms, from two and three transverse spatial mode families respectively, need to be loaded on SLM2. The values of QBER are $Q^{d=2}_{\text{BB84}} = 1.23\%$ and $Q^{d=2}_{\text{six-state}} = 1.28\%$, respectively corresponding to secure key rates of $R^{d=2}_{\text{BB84}} = 0.8086$ and $R^{d=2}_{\text{six-state}} = 0.8326$. The QBER mainly comes from experimental imperfections, such as the projective measurement. Note that the MPUBs protocol is the same as the BB84 protocol in the two-dimensional case, consisting of two MUBs as shown in figure 3(a). The matrix is obtained by the second measurement scheme with an average QBER $Q^{d=2}_{\text{MPUBs}} = 1.225\%$. Only two LG modes $\{|1,0\rangle, |-1,0\rangle\}$ need to be loaded on SLM2, indicating that the scheme reduces experimental resources. Because the cost and weight of passive devices are apperently lower than that of detectors, this is significant in specific application scenarios, such as satellites and drone platforms.

The reduced resource requirements allow us to perform higher-dimensional QKD. Figure 4 shows the crosstalk matrices obtained for MPUBs protocol with the second measurement setup in dimensions of $d = 4, 5, 6$. The number of holograms required to be loaded onto SLM2 is no more than six, which is a fair comparison to the two-dimensional protocols. The theory results are also presented for comparison. It is evident that when the basis settings are the same, diagonal elements can observe strong correlations. In performing the projective measurements, a completely orthogonal measurement state results in no correlations. Different from the MUBs-based protocols where the overlap between different basis is $1/d$, the overlap in MPUBs protocol $\{|\langle l_i'|h_j\rangle|^2, |\langle h_i'|l_j\rangle|^2\}$ is nonuniform, as shown in figures 4(a)–(c). The values of

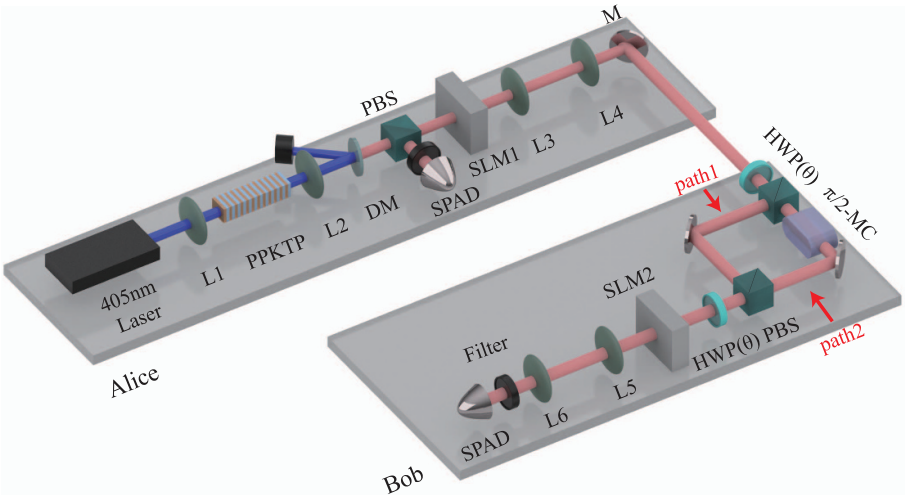

Figure 2. Experimental implementation of the MPUBs protocol. Periodically poled potassium titanyl phosphate (PPKTP); lens (L1-L6); dichroic mirror (DM); PBS; HWP; spatial light modulator (SLM); integrated $\pi/2$ mode converter ($\pi/2$-MC); mirror (M); high-pass optical filter (Filter); single-photon avalanche detector (SPAD).

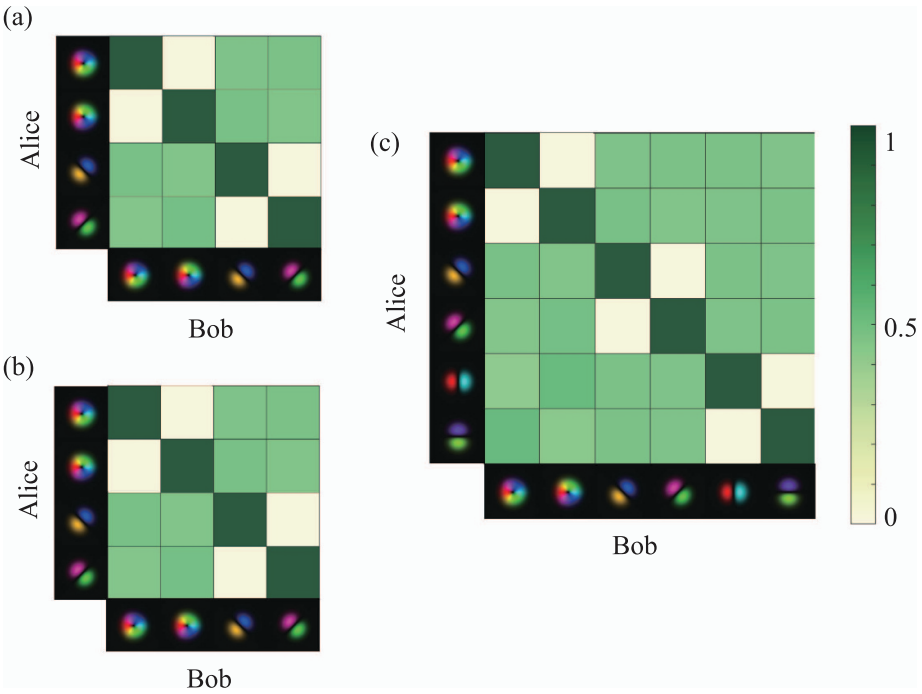

Figure 3. (a) The crosstalk matrix for two-dimensional MPUBs protocol based on the compact measurement scheme. (b) The crosstalk matrix for BB84 protocol based on the passive measurement scheme with the encoding states $\{|l_i\rangle, |h_i\rangle\}^{d=2}$. (c) The crosstalk matrix for six-state protocol based on the passive measurement scheme with the encoding states $\{|l_i\rangle, |h_i\rangle, (|l_i\rangle \pm |l_{j\neq i}\rangle)/\sqrt{2}\}^{d=2}$.

average fidelity obtained in experiments are $F^{d=4}_{\text{MPUBs}} = 96.76\%$, $F^{d=5}_{\text{MPUBs}} = 96.22\%$ and $F^{d=6}_{\text{MPUBs}} = 95.79\%$, benefiting from a large mode spacing. The discrepancy with theoretical results comes from noise, including imperfections in the projection measurements [52] and system misalignment. Both the unaligned and imperfect phase shift of the mode converter causes the upper right corner data to deviate more severely compared to the lower left corner data. Since the data where Alice and Bob select different bases are discarded in the sifting process, only the diagonal data obtained from the experiments are used to calculate the key rate. To calculate the practical key rates of the high-dimensional MPUBs protocol, we further consider the basis-dependent detection flaw introduced by the imperfect controlled unitary transformation.

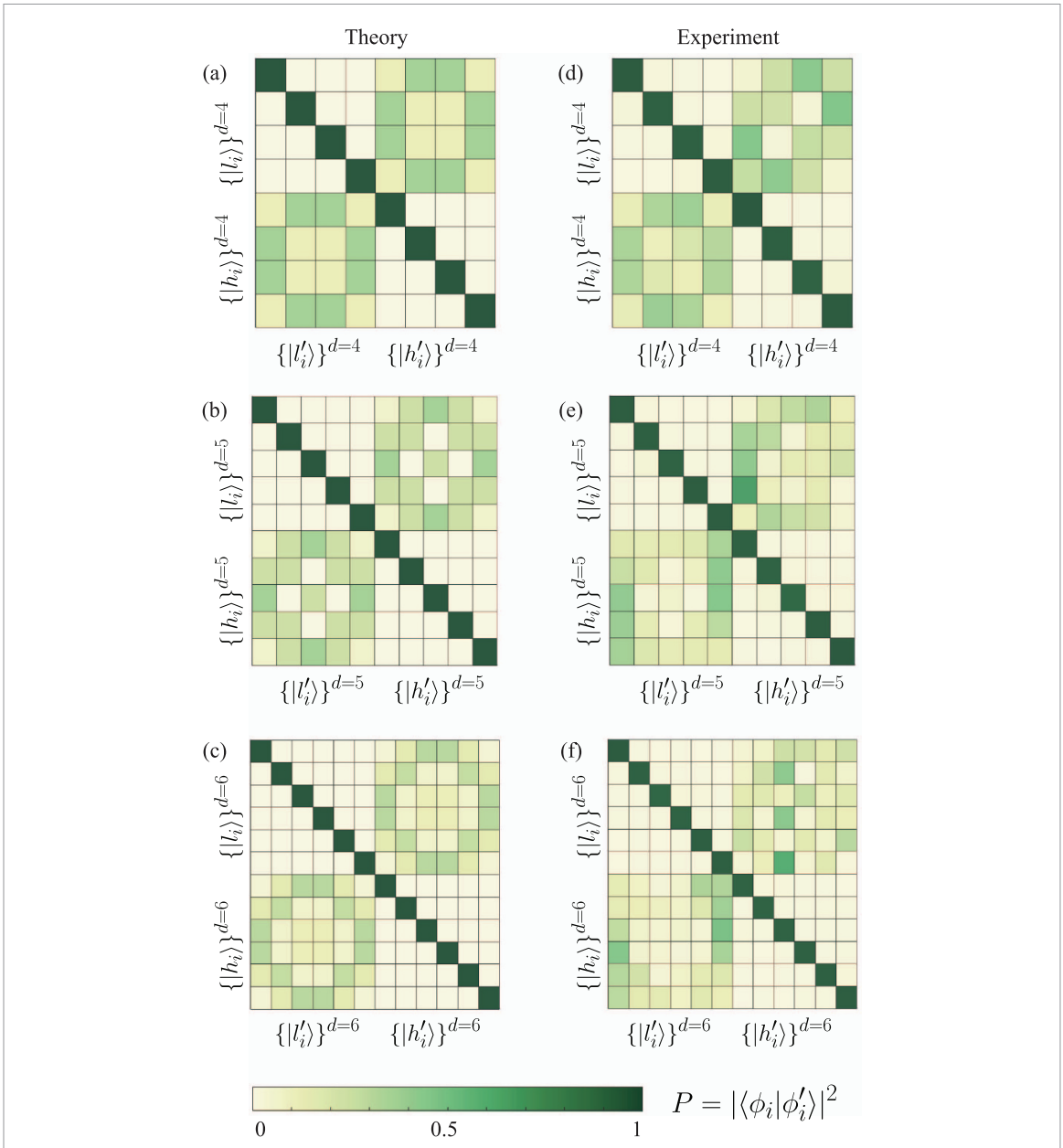

Figure 4. Experimental results for the MPUBs protocol in dimensions of $d = 4, 5, 6$. (a)–(c) The theoretical crosstalk matrices. (d)–(f) The experimental crosstalk matrices. $|\phi_i\rangle = \{|l_i\rangle, |h_i\rangle\}$ and $|\phi'_i\rangle$ represent the Alice's encoding and Bob's decoding states.

4. Practical security analysis

Existing QKD systems rely on an additional assumption that is hard to satisfy in practice: they require the devices used to distribute the key to be trusted [1]. In practical QKD systems, there will always be imperfections, Eve may learn some information about the key if Alice and Bob are not aware of or accurately characterize these imperfections. The practical security of QKD systems with a large variety of imperfections has been discovered and overcome in the past few years [5]. However, most works focus on two-dimensional systems, as the complexity of high-dimensional systems makes analysis technical.

In the transverse spatial mode encoding protocols, the detection system generally requires different settings of the mode sorter for each basis. And the settings are usually composed of multiple devices and maintaining balanced efficiency is not easy. In our scheme, an imbalance also exists due to a transmission loss of mode converter. This imperfection is known as the basis-dependent detection flaw. In addition, Bob also needs to consider the detection efficiency mismatch due to different detectors, which we ignore as only one detector is used in our proof-of-principle experiment.

For simplicity, we consider a general high-dimensional BB84-like protocols based on a single photon source. The first basis is given by the OAM basis which is a subset of spatial modes, i.e. $|\psi_i\rangle \in \{-d/2, \ldots, d/2\}$ and the second basis is generally given by the Fourier basis where the states are obtained from the

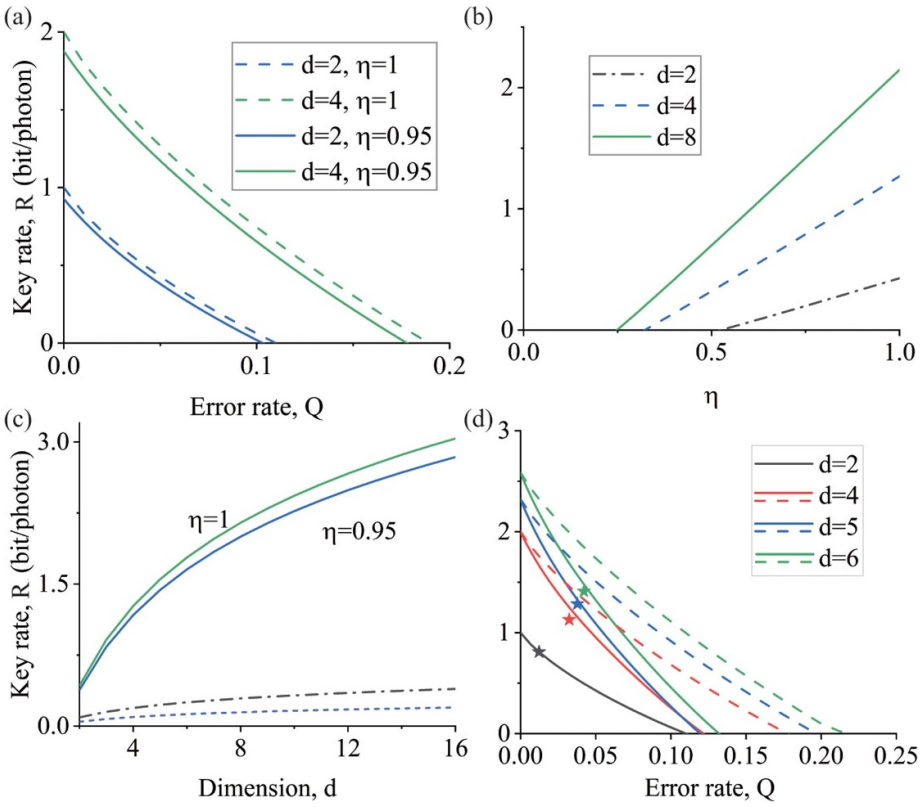

Figure 5. (a) The key rate bounds as a function of error rate Q for different dimensions. (b) The key rate bounds as a function of mode-dependent absorption η for different dimensions where the error rate is set to 0.05; (c) The key rate bounds as a function of dimension d for different η. Black dash-dot and blue dash curves represent the reduced key rates when $\eta = 0.9$ and 0.95, respectively. The error rate is set to 0.05. (d) Key rates of the MPUBs protocol. The solid lines are the theoretical results of the MPUBs protocol, which are lower than the MUBs-based protocol (dashed lines). The stars represent the experimental results. The key rates are lower than the curves due to the basis-dependent detection flaw.

discrete Fourier transform, $|\varphi_j\rangle = \frac{1}{\sqrt{d}} \sum_{j=0}^{d-1} \omega_d^{ij} |\psi_i\rangle$, with $\omega_d = \exp(i2\pi/d)$. A general detection setting similar as the left figure in figure 1(c). A 50 : 50 BS is used to select the measurement basis passively. Then two different mode sorters are applied to fully discriminate quantum states in a specific dimension. Assuming an extra, mode-independent absorption η exists when Bob measured on the Fourier basis. The secret key rate becomes [35]:

$$R \geqslant -h(Q) + \eta[\log_2 d - h(Q/\eta)], \tag{6}$$

which does not require the squashing model assumption and can be applied to any basis-dependent linear optical imperfections. Figures 5(a)–(c) show the effects of basis-dependent detection flaw in high-dimensional systems. The key rate drops overall in different dimensions and the maximum acceptable error rate decreases. Accurately characterizing this flaw is notably essential for determining the moment to abort the protocol. Meanwhile, high-dimensional protocols also show stronger resistance to the flaw, however, a protocol will suffer from more punishment along with the increase of dimension under the same η. Therefore, this flaw has an important impact on the scalability of the encoding dimension.

In our scheme, the mode converter has an average transmission efficiency of 91.62% at 810 nm. Most losses occur due to reflections from glass substrates, which can be eliminated by an anti-reflection coating, thereby overcoming the basis-dependent detection flaw. Our measurement scheme can be further improved by employing liquid crystal films coated on the mode converter to realize the conversion of polarization-selective response [53]. This improvement will allow overcome the basis-dependent detection flaw fundamentally. The final key rates for MPUBs protocol using a numerical method [54] shows in figure 5(d) by considering the flaw. The values of key rates are $R_{\mathrm{MPUBs}}^{d=4} = 1.1282$, $R_{\mathrm{MPUBs}}^{d=5} = 1.2846$ and $R_{\mathrm{MPUBs}}^{d=6} = 1.4092$, respectively, corresponding to the maximum transmission distance of around 75 km [55, 56]. It is evident that our scheme can increase the key rates by increasing the encoding dimension, even considering the detection flaw. Therefore, this scheme enhances robustness to system imperfections as well as environmental noise.

5. Discussion

Overall, we present a compact implementation of MPUBs protocol with the advantage that only requires one-half of mode sorters and detectors. In other words, the scheme allows doubling the encoding dimension under the same number of detectors. We experimentally demonstrate the protocol in dimensions of $d = 2, 4, 5$ and 6. The practical key rates obtained for the MPUBs protocol at $d = 4$ and $d = 6$ are 1.40 and 1.69 times higher than for the BB84 and six-state protocols, respectively. Note that the scheme is also feasible at the source side, allowing a high-speed generation of states in combination with mature HG mode lasers [57]. This compact implementation will benefit the applications of high-dimensional QKD in satellites and drone platforms, or connecting end-users to network nodes.

Data availability statement

The data that support the findings of this study are available upon reasonable request from the authors. All data that support the findings of this study are included within the article (and any supplementary files).

Acknowledgments

This work was supported by the National Nature Science Foundation of China (Grant Nos. 11804271, 12174301 and 91736104), the State Key Laboratory of applied optics and the Natural Science Basic Research Program of Shaanxi (Program No. 2023-JC-JQ-01).

Conflict of interest

The authors declare that they have no conflict of interest.

ORCID iDs

Zehong Chang https://orcid.org/0000-0002-2907-3495
Rui Qu https://orcid.org/0000-0001-7211-6078
Pei Zhang https://orcid.org/0000-0003-4523-4823

References

[1] Scarani V, Bechmann-Pasquinucci H, Cerf N J, Dušek M, Lütkenhaus N and Peev M 2009 *Rev. Mod. Phys.* **81** 1301
[2] Lo H K, Curty M and Tamaki K 2014 *Nat. Photon.* **8** 595–604
[3] Diamanti E, Lo H K, Qi B and Yuan Z 2016 *npj Quantum Inf.* **2** 1–12
[4] Wehner S, Elkouss D and Hanson R 2018 *Science* **362** eaam9288
[5] Xu F, Ma X, Zhang Q, Lo H K and Pan J W 2020 *Rev. Mod. Phys.* **92** 025002
[6] Portmann C and Renner R 2022 *Rev. Mod. Phys.* **94** 025008
[7] Cristiani I *et al* 2022 *J. Opt.* **24** 083001
[8] Bechmann-Pasquinucci H and Tittel W 2000 *Phys. Rev.* A **61** 062308
[9] Cerf N J, Bourennane M, Karlsson A and Gisin N 2002 *Phys. Rev. Lett.* **88** 127902
[10] Ecker S *et al* 2019 *Phys. Rev.* X **9** 041042
[11] Cozzolino D, Da Lio B, Bacco D and Oxenløwe L K 2019 *Adv. Quantum Technol.* **2** 1900038
[12] Yao A M and Padgett M J 2011 *Adv. Opt. Photonics* **3** 161–204
[13] Shen Y, Wang X, Xie Z, Min C, Fu X, Liu Q, Gong M and Yuan X 2019 *Light Sci. Appl.* **8** 90
[14] Erhard M, Fickler R, Krenn M and Zeilinger A 2018 *Light Sci. Appl.* **7** 17146–17146
[15] Erhard M, Krenn M and Zeilinger A 2020 *Nat. Rev. Phys.* **2** 365–81
[16] Restuccia S, Giovannini D, Gibson G and Padgett M 2016 *Opt. Express* **24** 27127–36
[17] Ndagano B, Mphuthi N, Milione G and Forbes A 2017 *Opt. Lett.* **42** 4175–8
[18] Nape I, Otte E, Vallés A, Rosales-Guzmán C, Cardano F, Denz C and Forbes A 2018 *Opt. Express* **26** 26946–60
[19] Zahidy M *et al* 2022 *AVS Quantum Sci.* **4** 011402
[20] Qu R, Wang Y, An M, Wang F, Quan Q, Li H, Gao H, Li F and Zhang P 2022 *Phys. Rev. Lett.* **128** 240402
[21] Qu R, Wang Y, Zhang X, Ru S, Wang F, Gao H, Li F and Zhang P 2022 *Optica* **9** 473–8
[22] Sit A *et al* 2017 *Optica* **4** 1006–10
[23] Cozzolino D *et al* 2019 *Phys. Rev. Appl.* **11** 064058
[24] Bouchard F *et al* 2018 *Opt. Express* **26** 22563–73
[25] Zhao J, Mirhosseini M, Braverman B, Zhou Y, Rafsanjani S M H, Ren Y, Steinhoff N K, Tyler G A, Willner A E and Boyd R W 2019 *Phys. Rev.* A **100** 032319
[26] Padgett M J, Miatto F M, Lavery M P, Zeilinger A and Boyd R W 2015 *New J. Phys.* **17** 023011
[27] Feng S and Winful H G 2001 *Opt. Lett.* **26** 485–7
[28] Hiekkamäki M, Barros R F, Ornigotti M and Fickler R 2022 *Nat. Photon.* **16** 828–33
[29] Vest G, Freiwang P, Luhn J, Vogl T, Rau M, Knips L, Rosenfeld W and Weinfurter H 2022 *Phys. Rev. Appl.* **18** 024067
[30] Wang Z, Malaney R and Burnett B 2020 *Phys. Rev. Appl.* **14** 064031
[31] Liu H Y *et al* 2021 *Phys. Rev. Lett.* **126** 020503

[32] Wang F et al 2020 Phys. Rev. A 101 032340
[33] Pirandola S et al 2020 Adv. Opt. Photonics 12 1012–236
[34] Wang F X, Chen W, Yin Z Q, Wang S, Guo G C and Han Z F 2019 Phys. Rev. Appl. 11 024070
[35] Lydersen L and Skaar J 2010 Quantum Inf. Comput. 10 60–76
[36] Berkhout G C, Lavery M P, Courtial J, Beijersbergen M W and Padgett M J 2010 Phys. Rev. Lett. 105 153601
[37] Mirhosseini M, Malik M, Shi Z and Boyd R W 2013 Nat. Commun. 4 2781
[38] Zhou Y, Mirhosseini M, Fu D, Zhao J, Rafsanjani S M H, Willner A E and Boyd R W 2017 Phys. Rev. Lett. 119 263602
[39] Gu X, Krenn M, Erhard M and Zeilinger A 2018 Phys. Rev. Lett. 120 103601
[40] Fu D et al 2018 Opt. Express 26 33057–65
[41] Fontaine N K, Ryf R, Chen H, Neilson D T, Kim K and Carpenter J 2019 Nat. Commun. 10 1865
[42] Zhou Y, Zhao J, Shi Z, Rafsanjani S M H, Mirhosseini M, Zhu Z, Willner A E and Boyd R W 2018 Opt. Lett. 43 5263–6
[43] Beijersbergen M W, Allen L, Van der Veen H and Woerdman J 1993 Opt. Commun. 96 123–32
[44] Jia J, Li Q, Zhang K, Chen D, Wang C, Gao H, Li F and Zhang P 2018 Appl. Opt. 57 6076–82
[45] Li S, Mo Q, Hu X, Du C and Wang J 2015 Opt. Lett. 40 4376–9
[46] Babazadeh A, Erhard M, Wang F, Malik M, Nouroozi R, Krenn M and Zeilinger A 2017 Phys. Rev. Lett. 119 180510
[47] Brandt F, Hiekkamäki M, Bouchard F, Huber M and Fickler R 2020 Optica 7 98–107
[48] Wang Y, Ru S, Wang F, Zhang P and Li F 2021 Quantum Sci. Technol. 7 015016
[49] Fung C H F, Tamaki K, Qi B, Lo H K and Ma X 2009 Quantum Inf. Comput. 9 131–65
[50] Mirhosseini M, Loaiza O S M, Chen C, Rodenburg B, Malik M and Boyd R W 2013 Opt. Express 21 30196–203
[51] Bouchard F, Valencia N H, Brandt F, Fickler R, Huber M and Malik M 2018 Opt. Express 26 31925–41
[52] Qassim H, Miatto F M, Torres J P, Padgett M J, Karimi E and Boyd R W 2014 J. Opt. Soc. Am. B 31 A20–A23
[53] Jia J, Zhang K, Hu G, Hu M, Tong T, Mu Q, Gao H, Li F, Qiu C W and Zhang P 2021 Photon. Res. 9 1048–54
[54] Chang Z, Wang F, Jia J, Wang X, Lv Y and Zhang P 2022 J. Opt. Soc. Am. B 39 2823–30
[55] Wang W, Xu F and Lo H K 2018 Phys. Rev. A 97 032337
[56] Wang X, Wu T, Dong C, Zhu H and Zhao S 2021 Photon. Res. 9 B9–B17
[57] Pan J, Shen Y, Wan Z, Fu X, Zhang H and Liu Q 2020 Phys. Rev. Appl. 14 044048